Mice Lacking the Neuropeptide α-Calcitonin Gene-Related Peptide Are Protected Against Diet-Induced Obesity

Christopher S. Walker, Xiaoling Li, Lynda Whiting, Sarah Glyn-Jones, Shaoping Zhang, Anthony J. Hickey, Mary A. Sewell, Katya Ruggiero, Anthony R. J. Phillips, Edward W. Kraegen, Debbie L. Hay, Garth J. S. Cooper, and Kerry M. Loomes

School of Biological Sciences (C.S.W., X.L., L.W., S.G.-J., S.Z., A.J.H., M.A.S., K.R., A.R.J.P., D.L.H., G.J.S.C., K.M.L.), Maurice Wilkins Centre for Molecular Biodiscovery (C.S.W., A.J.H., A.R.J.P., D.L.H., G.J.S.C., K.M.L.), Faculty of Science, and Department of Surgery (A.R.J.P.), Faculty of Medical and Health Sciences, University of Auckland, Auckland 1142, New Zealand; Diabetes and Obesity Research Program (E.W.K.), Garvan Institute of Medical Research, Sydney NSW 2010, Australia; and Department of Pharmacology (G.J.S.C.), Medical Sciences Division, University of Oxford, Oxford OX1 3 QT, United Kingdom

α-Calcitonin gene-related peptide (αCGRP) is a neuropeptide that is expressed in motor and sensory neurons. It is a powerful vasodilator and has been implicated in diverse metabolic roles. However, its precise physiological function remains unclear. In this study, we investigated the role of αCGRP in lipid metabolism by chronically challenging αCGRP-specific knockout ($\alpha CGRP^{-/-}$) and control mice with high-fat diet regimens. At the start of the study, both animal groups displayed similar body weights, serum lipid markers, and insulin sensitivity. However, $\alpha CGRP^{-/-}$ mice displayed higher core temperatures, increased energy expenditures, and a relative daytime (nonactive) depression in respiratory quotients, which indicated increased β-oxidation. In response to fat feeding, $\alpha CGRP^{-/-}$ mice were comparatively protected against diet-induced obesity with an attenuated body weight gain and an overall reduction in adiposity across all the three diets examined. $\alpha CGRP^{-/-}$ mice also displayed improved glucose handling and insulin sensitivity, lower im and hepatic lipid accumulation, and improved overall metabolic health. These findings define a new role for αCGRP as a mediator of energy metabolism and opens up therapeutic opportunities to target CGRP action in obesity. **(*Endocrinology* 151: 4257–4269, 2010)**

Calcitonin gene-related peptide (CGRP) is a 37 amino acid neuropeptide that is expressed primarily in motor and sensory neurons in both central and peripheral nervous systems. CGRP belongs to the calcitonin peptide family and is characterized by two posttranslational modifications that are important for activity, and which comprise an amidated C terminus and a cyclic N terminus formed through a disulfide bridge (1). Two distinct homologs, αCGRP and βCGRP, have been identified, which differ by three amino acids in humans and by one amino acid in rodents (2). αCGRP and calcitonin are derived via tissue-specific alternative splicing of the primary transcript of the *CALCA* gene (3), whereas βCGRP is the sole product encoded by a distinct *CALCB* gene (4).

Both αCGRP and βCGRP and their binding sites, are widely distributed throughout the central nervous system,

ISSN Print 0013-7227 ISSN Online 1945-7170
Printed in U.S.A.

doi: 10.1210/en.2010-0284 Received March 9, 2010. Accepted June 3, 2010.
First Published Online July 7, 2010

Abbreviations: ACC, Acetyl coenzyme A carboxylase; ALP, alkaline phosphatase; ALT, alanine transaminase; AMPK, AMP-activated protein kinase; AUC, area under the curve; CGRP, calcitonin gene-related peptide; $\alpha CGRP^{-/-}$, αCGRP knockout; $\alpha CGRP^{+/+}$, αCGRP control; CS, citrate synthase; fT3, free triiodothyronine; fT4, free thyroxine; GTT, glucose tolerance test; 3-HAD, 3-hydroxyacyl coenzyme A dehydrogenase; H&E, hematoxylin and eosin; ITT, insulin tolerance test; LME, linear mixed effects; pACC, phosphorylated ACC; PAI-1, plasminogen activator inhibitor; pAMPK, phosphorylated AMPK; REML, restricted maximum likelihood; RQ, respiratory quotient; TRPV1, transient receptor potential vanilloid 1; TSH, thyroid-stimulating hormone.

including the hypothalamus, cerebellum, and spinal cord (5–7). In the periphery, the β-isoform is expressed predominantly in enteric neurons of the gut (8), whereas αCGRP is colocalized with the classical neurotransmitter acetylcholine in cranial as well as spinal motoneurons (9, 10). CGRP is also expressed in Aδ- and C-fiber sensory nerve populations, where its release from various tissues, including skeletal muscle (11), is stimulated via activation of the transient receptor potential vanilloid 1 (TRPV1) (12).

αCGRP is a potent vasodilator with widespread tissue distribution (13). Interestingly, CGRP has been implicated in biological roles by virtue of roles in insulin resistance (14), food intake (15), cardiovascular conditioning (16), neuromuscular junction biology (17), immune regulation (18), and regulation of sympathetic outflow (19). However, the physiological importance of CGRP in several of these processes still remains unclear in the light of previous studies on knockout mice lines lacking expression of αCGRP. Although some effects have been found in sympathetic activity (20) and bone homeostasis (21), mice otherwise exhibit apparently normal cardiovascular regulation and neuromuscular development (22).

We showed previously that acute incubation of isolated rat soleus muscle with exogenous αCGRP (100 nM) stimulated muscle lipolysis with associated activation of AMP-activated protein kinase (AMPK) and β-oxidation to a level comparable with maximal 5-aminoimidazole-4-carboxamide-1-β-ribofuranoside and adiponectin stimulation (23). However, it is still uncertain as to whether these metabolic actions of CGRP on AMPK activation and β-oxidation represent physiological or pharmacological phenomena. On the basis of these findings, we proposed that αCGRP released from sensory or motor neurons (11) may regulate lipid metabolism.

To directly investigate the role of αCGRP in lipid homeostasis within a physiological context, we investigated a specific αCGRP knockout (αCGRP$^{-/-}$) model, in which the *Calca* gene has been modified to lack CGRP expression while retaining normal calcitonin expression (21, 22). Despite an absence of any obvious phenotype (22), this model remains uncharacterized with respect to lipid handling. In this study, we chronically challenged αCGRP$^{-/-}$ and αCGRP control (αCGRP$^{+/+}$) mice with two high-fat diet regimens. The mice were assessed for body weight and metabolic status. These data demonstrate that αCGRP$^{-/-}$ mice were protected from diet-induced obesity, which was associated with increased energy expenditure, improved metabolic health, and insulin sensitivity. These findings define a role for αCGRP in metabolic regulation and lipid management.

Materials and Methods

Animals

C57BL/6 control (αCGRP$^{+/+}$) and αCGRP$^{-/-}$ mice were kindly provided by Ronald Emerson, Vanderbilt University School of Medicine (Nashville, TN) (22). αCGRP$^{-/-}$ mice were backcrossed into the C57BL/6 background for at least 10 generations before these studies and maintained as separate homozygous and wild-type lines. Mice pairs were housed in a controlled environment (12-h light, 12-h dark cycle; room temperature, 22 ± 2 C) with *ad libitum* access to food and water. All procedures involving the use of animals were approved by the University of Auckland Animal Ethics Committee. All experiments were performed in male mice.

Before entry into these studies, all mice were maintained on a standard colony diet (Teklad TB 2018; Harlan, Madison, WI). Male mice between 39 and 45 d old and weighing between 19 and 23 g were recruited into either a baseline or fat-feeding study. For the baseline study, mice were fed a control diet (10% fat, 12450B; Research Diets, New Brunswick, NJ) for 10 d (≥49 d of age) before being killed. For the fat-feeding study, mice were fed either a control 10% fat diet, a 45% fat diet (12451; Research Diets), or a 60% fat diet (12492; Research Diets) for 182 d (~224 d of age) before killing. Bodyweight and nonfasted blood glucose measurements were performed weekly. Total food intake was calculated as the weight of food lost from the "food hopper." For both the baseline study and the fat-feeding study, brief terminal anesthesia was induced with 5% isoflurane in 2 liter/min O_2 and maintained on 2% isoflurane in 2 liter/min O_2. Blood was collected directly from the vena cava. Mice were killed via cervical dislocation while anesthetized. Tissues were collected, weighed, and snap frozen in liquid N_2 or processed for histological analysis.

Western blot analysis

Total protein was isolated from liver or red quadriceps muscle in extraction buffer [20 mM Tris-HCl (pH 7.4), 1% Triton X-100, 50 mM NaCl, 250 mM sucrose, 50 mM NaF, and 5 mM sodium pyrophosphate] and a protease inhibitor cocktail (Roche, Basel, Switzerland); 50 μg of liver protein or 30 μg of red quadriceps muscle protein were then separated by SDS-PAGE.

Hepatic morphology

Approximately 5-mm^2 fresh liver samples were placed in standard cryo-molds and covered in Tissuetek OCT compound (Sakura Finetek, Inc., Tokyo, Japan). Tissues were then snap frozen in liquid N_2-precooled isopentane. Frozen sections were cut at −20 C using a Leica Cryocut 1850 Cryomicrotome and stained with either hematoxylin and eosin (H&E) (6 μM sections) or Oil red-O (12-μM sections).

Glucose tolerance test (GTT) and insulin tolerance test (ITT)

GTTs and ITTs, performed 7 d (or 4 d in the baseline study) after the GTTs, were performed after a 4-h fast. Glucose (1 g/kg; David Bull Laboratories, Lidcombe, Australia) or insulin (1 U/kg; Actrapid, Novo Nordisk Pharmaceuticals Ltd., Bagsværd, Denmark), was administered into the ip cavity and blood glucose measured (Accu-Chek).

Temperature distribution

A lubricated 2-mm rectal thermometer was inserted approximately 10 mm inside the rectal cavity and the temperature recorded. Core body temperature was measured 2–5 d before the end of either baseline or fat-feeding portions of the studies (same room between 0900 and 1100 h, ambient temperature-controlled room 19–21 C, two nonconsecutive days with the two measurements averaged). Surface body temperature was measured at a similar time and conditions as the rectal temperatures. Thermal images were then taken from 40 cm above the mice and maximum surface temperature recorded from these images with a Ti30 thermal imaging camera (Fluke Corp., San Diego, CA).

Indirect calorimetry and locomotor activity

Indirect calorimetry was performed in 42- to 49-d-old $\alpha CGRP^{+/+}$ or $\alpha CGRP^{-/-}$ mice using an open-circuit system of the Comprehensive Laboratory Animal Monitoring System (Columbus Instruments, Columbus, OH).

Mitochondrial enzyme activities

Enzymatic activities of citrate synthase (CS) and 3-hydroxyacyl coenzyme A dehydrogenase (3-HAD) were measured spectrophotometrically in liver, red quadriceps muscle, and epididymal adipose tissue homogenates. Briefly, 20–50 mg of frozen tissue were homogenized in a 1:10 volume (wt/vol) of ice-cold homogenization buffer [100 mmol/liter^{-1} Tris-HCl (pH 7.5)] using an Ultra Turrax homogenizer (IKA, Staufen, Germany) and assayed as described previously (24). Data collection was performed on a SpectraMax 340 plate reader (Molecular Devices, Sunnyvale, CA) and normalized to wet tissue weight.

Serum metabolites and hormones

Serum cholesterol, free fatty acid, high-density lipoprotein, alkaline phosphatase (ALP), alanine transaminase (ALT), aspartate transaminase, total protein, and triglyceride tests were performed on a Synchron CX5CE (Beckham Coulter, Inc., Brea, CA). Serum insulin, IL-6, leptin, monocyte chemotactic protein-1, total plasminogen activator inhibitor (PAI-1), resistin, and TNF-α were measured using a commercially available kit (mouse serum adipokine lincoplex kit; Millipore Corp., Bedford, MA). Serum adiponectin and thyroid-stimulating hormone (TSH) were measured using ELISA kits [mouse serum adiponectin ELISA (Millipore Corp.) and mouse TSH ELISA, AKRTS-010E; Shibayagi Co., Ltd., Gunma, Japan)]. Free triiodothyronine (fT3) and free thyroxine (fT4) were measured using EIA kits (fT3 EIA kit and fT4 EIA kit; Diagnostic Systems Laboratories, Inc., Webster, TX).

Tissue triglyceride determination

Red quadriceps muscle and liver triglyceride were measured using an Iatroscan Mark V^{new} thin-layer chromatography/flame ionization detection system and a triple development as described in Sewell (25).

Statistics and data analysis

All data are expressed as mean ± SEM. Statistical analyses were performed using GraphPad Prism version 4.2 (GraphPad Software, San Diego, CA) for unpaired two-tailed *t* tests and SAS version 9.1 (SAS institute, Cary, NC) or S-PLUS (Tibco Software, Palo Alto, CA) for two-way ANOVA and linear mixed effects (LME) models fit using restricted maximum likelihood (REML). The precise methods used are described in the figure legends. $P < 0.05$ was considered statistically significant.

Results

$\alpha CGRP^{-/-}$ mice displayed increased core body temperature

Analyses undertaken on animals from the baseline study (≥49 d of age) showed a lower surface (~0.5 C; $P < 0.05$) and higher core temperature (by ~1 C; $P < 0.05$) in $\alpha CGRP^{-/-}$ mice compared with $\alpha CGRP^{+/+}$ mice (Fig. 1A). This difference was not observed during the final week (between d 217 and 219) of the fat-feeding study (data not shown). Analyses of individual organ weights from the baseline study showed that $\alpha CGRP^{-/-}$ mice had approximately 27% lighter epididymal fat pads, and approximately 21 and 10% heavier spleen and liver weights, respectively (Supplemental Table 1, published on The Endocrine Society's Journals Online web site at http://endo.endojournals.org). Soleus muscle, inguinal, and mesenteric fat pad weights did not differ. Corresponding analyses of serum metabolites showed an approximate 9% reduction ($P < 0.05$) in total cholesterol concentration in $\alpha CGRP^{-/-}$ mice but no differences in either triglyceride or free fatty acid concentrations (Supplemental Table 1). There were no significant differences in the thyroid hormones, TSH and fT4, or fT3.

$\alpha CGRP^{-/-}$ mice were protected against diet-induced obesity

For the fat-feeding study, $\alpha CGRP^{-/-}$ or $\alpha CGRP^{+/+}$ mice were each randomized into one of three groups and administered either the control 10% diet, 45 or 60% fat diets until 224 d of age. Throughout the study, weekly body weight measurements were recorded. Mean body weights upon entry to the fat-feeding study for each of the six experimental groups did not differ significantly (Fig. 1B). The contribution of diet, age, and genotype to the growth curve trajectories was analyzed using a LME model fit using REML. A significant interaction between age and diet was identified, showing that both $\alpha CGRP^{-/-}$ and $\alpha CGRP^{+/+}$ mice fed the 45% fat ($P < 0.0001$) and 60% fat ($P < 0.0001$) diets had greater rates of body weight gain compared with respective mice fed the control 10% fat diet. There was also a significant interaction between age and genotype ($P < 0.0001$) showing that $\alpha CGRP^{+/+}$ experienced a more rapid weight increase than $\alpha CGRP^{-/-}$ mice for all three diets. At the end of the fat-feeding study, mean body weights of $\alpha CGRP^{+/+}$ mice were 16, 12, and 9% heavier than $\alpha CGRP^{-/-}$ mice on the corresponding 10, 45, and 60% fat diets (Fig. 1B).

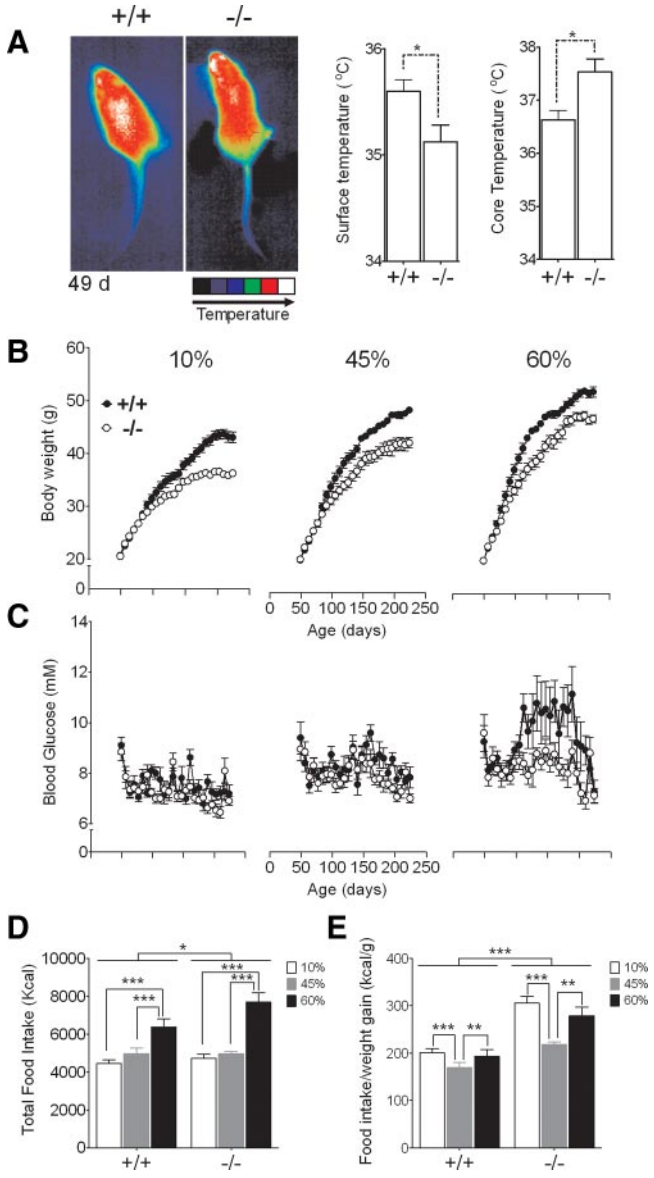

FIG. 1. αCGRP$^{-/-}$ mice exhibit a lean phenotype despite increased food intake. A, Surface (n = 6/group) and core body temperature (n = 12–14 mice/group) in mice at 49 d (baseline study). Representative images taken using a thermal imager are shown. Statistical significance was analyzed using unpaired Student's *t* test. All values are expressed as mean ± SEM. B, Weight and age-matched αCGRP$^{-/-}$ (*open circle*) and αCGRP$^{+/+}$ (*closed circle*) mice were fed from 42 d of age either a control 10% fat diet or one of two high-fat diets containing 45 or 60% calories from fat (fat-feeding study). Body weights were measured weekly and expressed as mean ± SEM (n = 12–14 mice/group). C, Corresponding blood glucose concentrations as measured weekly (n = 12–14 mice/group). Both the weight trajectories and blood glucose profiles were analyzed using a LME model fit using REML and revealed significant age ∗ diet ($P < 0.0001$) and genotype ∗ age interactions ($P < 0.0001$) for each of the three diets. D, Total food intake (n = 6–7 mice/group) over the period of 42–224 d. E, Total food intake normalized to weight gain over the period of 42–224 d (n = 6–7 mice/group). Statistical significance was analyzed by two-way ANOVA and Tukey-Kramer *post hoc* analyses. All values are expressed as mean ± SEM. *, $P < 0.05$; **, $P < 0.01$; ***, $P < 0.001$.

Fasting blood glucose was measured weekly during the fat-feeding study (Fig. 1C). At the start of the study, mean fasting glucose concentrations for each of the six experimental groups were not significantly different. However, statistical analyses revealed a significant interaction between age and genotype ($P < 0.0001$), revealing increasing divergence in blood glucose concentrations between αCGRP$^{+/+}$ and αCGRP$^{-/-}$ mice on the 45 and 60% fat diets. These findings showed that the lower rate of weight gain in the αCGRP$^{-/-}$ mice was associated with improved glucose homeostasis in response to high-fat feeding.

Cumulative food intake over the duration of the fat-feeding study was measured for each of the six experimental groups. Over this period, the total calorie intake of mice from both genotypes on the 60% fat diet was significantly higher than that of mice on the control 10% ($P < 0.001$) and 45% fat diet ($P < 0.001$). αCGRP$^{-/-}$ mice also showed a small yet significant increase in total food intake over this period compared with αCGRP$^{+/+}$ mice ($P < 0.05$) (Fig. 1D). This absolute increase in food intake for αCGRP$^{-/-}$ mice translated into an overall increased caloric intake when normalized for body weight gain over the study period and across all diets ($P < 0.001$) (Fig. 1E).

Analyses of final organ weights from the fat-feeding study at 224 d revealed a significant effect of dietary fat content ($P < 0.001$) to increase liver weight for both αCGRP$^{-/-}$ and αCGRP$^{+/+}$ mice (Supplemental Table 2). Nevertheless, livers weighed on average approximately 40% less in αCGRP$^{-/-}$ mice ($P < 0.001$) compared with their wild-type counterparts across the three diets. Mean spleen weight also mirrored this reduction (Supplemental Table 2). There were also significant genotype effects on adipose mass with overall lighter inguinal ($P < 0.001$) and mesenteric ($P < 0.01$) but not epididymal fat pad masses in αCGRP$^{-/-}$ compared with αCGRP$^{+/+}$ mice. Soleus muscles weighed significantly less ($P < 0.05$) in αCGRP$^{-/-}$ compared with αCGRP$^{+/+}$ mice.

αCGRP$^{-/-}$ mice displayed altered respiratory quotient (RQ) and increased energy expenditure

Indirect calorimetry of baseline mice revealed a divergence in both VO_2 (Fig. 2A) and VCO_2 (genotype ∗ time interaction, $P < 0.001$) (Fig. 2B). In particular, both parameters were higher in αCGRP$^{-/-}$ compared with αCGRP$^{+/+}$ mice with this difference first evident around the transition from dark to light period. These changes were reflected by apparently higher energy expenditure over the same period (genotype ∗ time interaction, $P < 0.05$) (Fig. 2C). αCGRP$^{-/-}$ mice also exhibited a decline in RQs, beginning at the 2-h active period and continuing for 1 h into the dark period, indicating a metabolic partitioning toward β-oxidation (genotype ∗ time interaction,

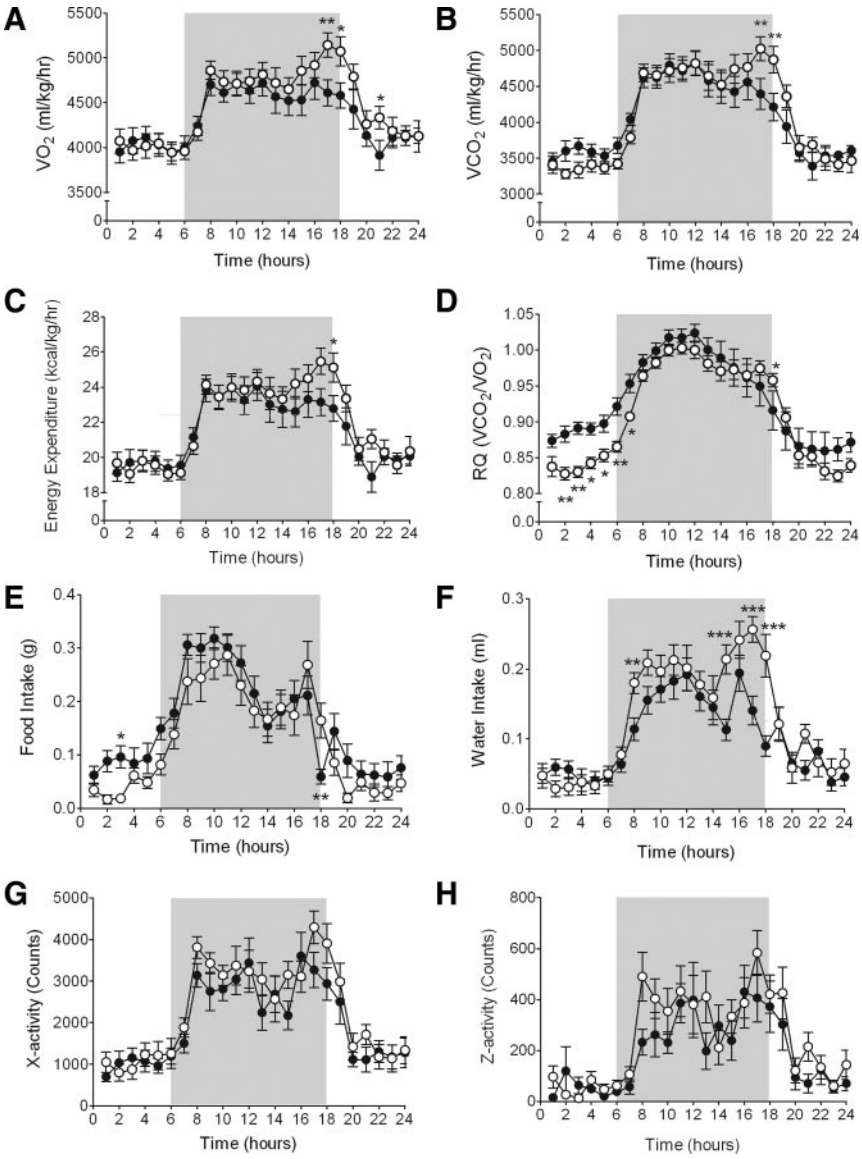

FIG. 2. Indirect calorimetry, feeding behavior, and locomotor activity in baseline $\alpha CGRP^{+/+}$ (*closed circle*) and $\alpha CGRP^{-/-}$ (*open circle*) mice. Male mice between 39 and 45 d old and weighing between 19 and 23 g were acclimated to respirometry chambers for approximately 72 h followed by a 24-h period of data collection. Chambers were equipped with two arrays of infrared beams for continuous measurement of X-activity (*horizontal*) and Z-activity (*vertical*). Infrared beam-breaks in both the x- and z-axes were quantified as counts. Studies were performed under a 12-h light, 12-h dark cycle at a room temperature of 22 ± 2 C. During this period, VO_2 (A), VCO_2 (B), energy expenditure (C), RQ (D), food intake (E), water intake (F), X-activity (G), and Z-activity (H) were measured. Values are expressed as mean ± SEM (n = 10–12 mice/group). Mean ± SEM body weights of $\alpha CGRP^{+/+}$ and $\alpha CGRP^{-/-}$ mice before acclimatization were 21.5 ± 0.5 g (n = 10) *vs.* 20.9 ± 0.3 g (n = 12, not significant), respectively. The dark cycle between 6 and 18 h is *shaded*. A repeated measures analysis using REML, assuming compound symmetry, was performed on the data (SAS version 9.1). Comparisons of *a priori* interest were contrasted and unadjusted *P* values are shown. *, $P < 0.05$; **, $P < 0.01$; ***, $P < 0.001$.

$P < 0.001$) (Fig. 2D). This was associated with possible variations in daily food intake (genotype * time interaction, $P < 0.05$) (Fig. 2E). There was increased water intake between 14 and 18 h in $\alpha CGRP^{-/-}$ mice (genotype * time interaction, $P < 0.001$) (Fig. 2F). There were no significant differences in physical activity over the 24-h period between the two groups (genotype * time interaction, not significant) (Fig. 2, G and H).

$\alpha CGRP^{-/-}$ mice displayed improvement in metabolic markers of obesity and insulin resistance

In the baseline study, there were no differences in glucose handling between $\alpha CGRP^{-/-}$ and $\alpha CGRP^{+/+}$ mice as analyzed by unpaired Student's *t* test on the total area under the curve (AUC) (data not shown). Intraperitoneal GTTs were performed in animals from the fat-feeding study at 119, 161, and 206 d (Fig. 3). Statistical analyses for the fat-feeding study (Supplemental Table 3) revealed, as expected, impaired glucose handling for both $\alpha CGRP^{-/-}$ and $\alpha CGRP^{+/+}$ mice fed either the 45% fat or 60% high-fat diets ($P < 0.0001$) compared with mice fed the control 10% diet. Importantly, the effect of diet was genotype dependent with more efficient glucose handling in $\alpha CGRP^{-/-}$ mice compared with $\alpha CGRP^{+/+}$ mice on the 45% ($P < 0.0001$) and 60% ($P < 0.0001$) diets at all time points except for the 60% fat diet at 206 d, where there was no difference. There was also a significant genotype difference on the control 10% diet at 206 d.

Intraperitoneal ITTs were performed at 126, 168, and 213 d (Fig. 4) and curves analyzed by total AUC for each of the three dietary groups (Supplemental Table 4). Overall, ipITT responses mirrored the differences observed for the ipGTT responses for both $\alpha CGRP^{-/-}$ and $\alpha CGRP^{+/+}$ mice with a decrease for either the 45% fat or 60% fat diets relative to the control 10% diet. However, the effect of diet was again genotype dependent with more efficient insulin handling in $\alpha CGRP^{-/-}$ mice, relative to $\alpha CGRP^{+/+}$ mice on the 45 and 60% fat diets at d 126 and 168. Otherwise, there were no genotype differences on the 10% diet at these two time points. At d 213, $\alpha CGRP^{-/-}$ mice displayed better insulin handling for both 10 and 45%. However, this effect was attenuated on the 60% diets at 213 d. Overall, these findings showed that $\alpha CGRP^{-/-}$ mice displayed improved

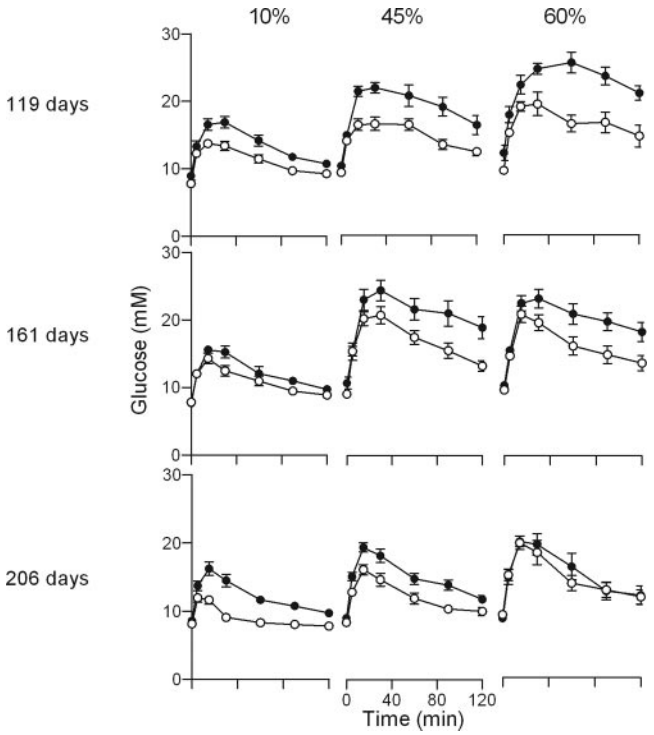

FIG. 3. αCGRP$^{-/-}$ mice display improved glucose handling. GTTs were sequentially performed at 119, 161, and 206 d on the same αCGRP$^{-/-}$ (*open circle*) or αCGRP$^{+/+}$ (*closed circle*) animal cohort from the fat-feeding study. Statistical analyses were performed on the total AUC using a LME model fit using REML and are summarized in Supplemental Table 3. Data are shown as mean ± SEM (n = 9–16 mice/group).

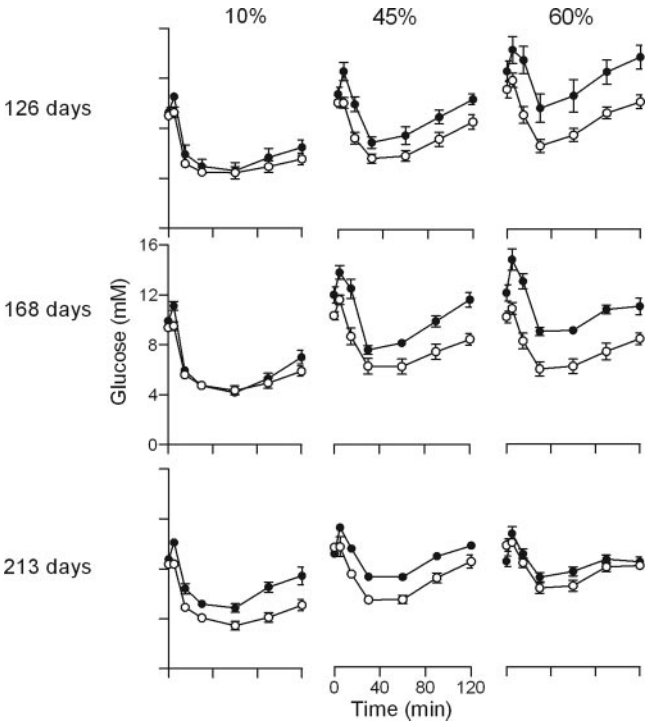

FIG. 4. αCGRP$^{-/-}$ mice display improved insulin tolerance. ITTs were sequentially performed at 126, 168, and 213 d on the same αCGRP$^{-/-}$ (*open circle*) or αCGRP$^{+/+}$ (*closed circle*) animal cohort from the fat-feeding study. Total AUC was analyzed using a LME model fit using REML as summarized in Supplemental Table 4. Data are shown as mean ± SEM (n = 10–16 mice/group).

glucose tolerance and insulin handling in response to fat feeding. The data also suggest that this improvement can be overcome by the extremes of high-fat diets and age.

In the baseline study, there was no difference between the serum insulin concentrations of αCGRP$^{-/-}$ and αCGRP$^{+/+}$ mice (Fig. 5A). However, in the fat-feeding study, there were increased serum insulin concentrations in both αCGRP$^{-/-}$ and αCGRP$^{+/+}$ mice on the 45% ($P < 0.05$) and 60% fat diets ($P < 0.01$) *vs.* the control 10% diet. There was also a significant genotype effect ($P < 0.01$), showing lower overall serum insulin concentrations in αCGRP$^{-/-}$ mice across the three diets (Fig. 5A).

Circulating levels of resistin were similar between 49-d-old (baseline study) and 224-d-old mice (fat-feeding study) fed the 10% fat diet (Fig. 5B). However, by 224 d, resistin levels were increased in αCGRP$^{-/-}$ mice administered either the 45 or 60% fat diets ($P < 0.01$) *vs.* the 10% fat diet and in αCGRP$^{+/+}$ mice administered the 60% fat diet ($P < 0.01$) *vs.* mice fed either the 10 or 45% fat diets (Fig. 5B). Serum leptin levels were also elevated in 224-d αCGRP$^{-/-}$ mice administered the 60% high-fat diet *vs.* 10% diet ($P < 0.001$) (Fig. 5C). The effect of diet was genotype dependent with a lower leptin serum concentration in αCGRP$^{-/-}$ mice compared with αCGRP$^{+/+}$ mice relative to the 10% fat diet ($P < 0.05$) (Fig. 5C). These dietary-induced increases in resistin and leptin concentrations occurred in the absence of significant differences in adiponectin concentrations (Supplemental Table 5).

For the baseline study, soleus muscle triglyceride content was not significantly different between genotypes at 49 d (Fig. 5D). However, lipid analyses taken at 224 d for the fat-feeding study showed significant triglyceride accumulation in the soleus muscle of both αCGRP$^{-/-}$ and αCGRP$^{+/+}$ mice on the 45% ($P < 0.001$) and 60% fat diets ($P < 0.001$) *vs.* the control 10% diet (Fig. 5D). There was also a genotype effect ($P < 0.001$), showing lower triglyceride content in αCGRP$^{-/-}$ mice across all diets. Overall, the leaner phenotype of αCGRP$^{-/-}$ mice was associated with improved glucose handling, improved insulin sensitivity, lower hyperinsulinemia, and a reduction in skeletal muscle triglyceride content.

Development of fatty liver induced by high-fat feeding was attenuated in αCGRP$^{-/-}$ mice

No gross differences in liver morphology were observed between αCGRP$^{-/-}$ and αCGRP$^{+/+}$ mice from the baseline study at 49 d, as indicated by H&E and Oil red-O staining (Fig. 6A). However, for the fat-feeding study, both animal groups showed fatty liver as a consequence of high-fat feeding. As described above, compared with αCGRP$^{+/+}$ mice, livers weighed approximately 40% less in αCGRP$^{-/-}$ mice

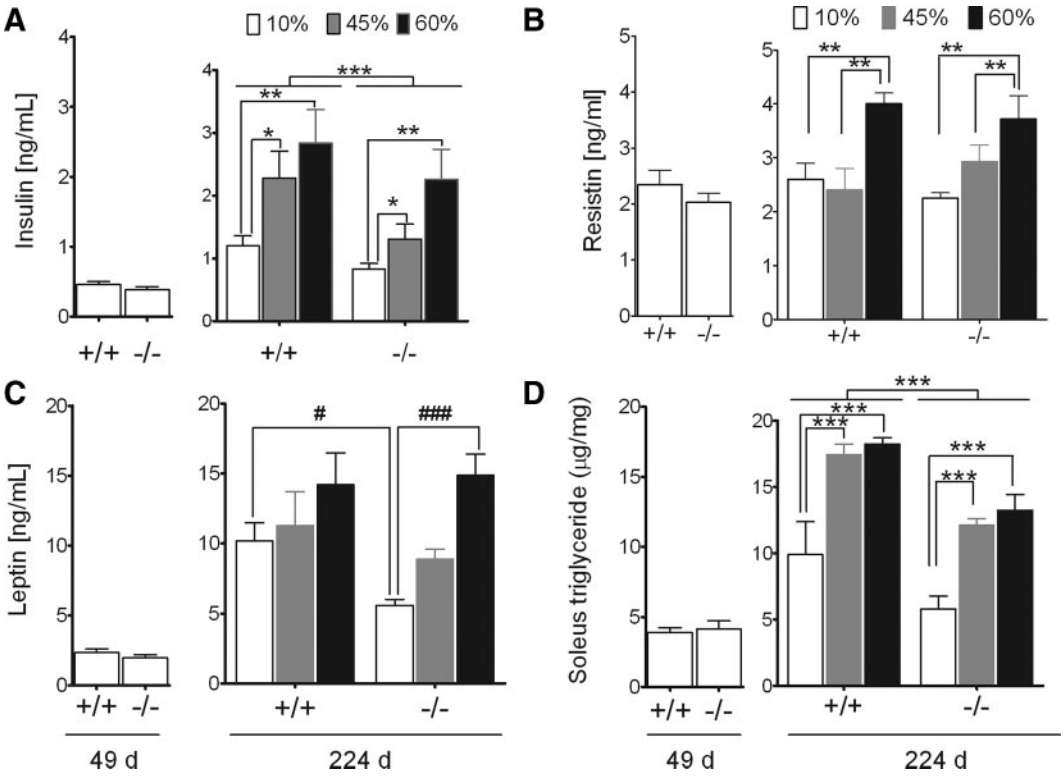

FIG. 5. The 224-d αCGRP$^{-/-}$ mice display improved levels of serum biomarkers associated with obesity. A, Serum insulin concentrations. B, Serum resistin concentrations. C, Serum leptin concentrations. D, Soleus muscle triglyceride content. Values are expressed as mean ± SEM (n = 9–12 mice/group, except soleus muscle, n = 5 mice/group). *, $P < 0.05$; **, $P < 0.01$; ***, $P < 0.001$. Analyses at 49 d were performed on a separate animal cohort (baseline study). Statistical analyses were performed using two-way ANOVA and where a significant genotype ∗ diet interaction was observed, the *post hoc* Tukey-Kramer tests are represented by *hashed symbols*. #, $P < 0.05$; #, $P < 0.001$.

(Supplemental Table 2). Further, H&E staining revealed the presence of lacunae in sections from both αCGRP$^{-/-}$ and αCGRP$^{+/+}$ mice, consistent with loss of lipid during the staining process; these appeared smaller and less dense in the livers derived from αCGRP$^{-/-}$ mice. Complementary Oil red-O staining confirmed this observation showing smaller and less dense globular droplets in αCGRP$^{-/-}$ mice livers (Fig. 6A). Lipid droplets were distributed in a focal diffuse manner that was more pronounced in αCGRP$^{-/-}$ mice and were associated with an apparent increase in pyknotic nuclei content.

Collectively, these observations suggested that lower lipid accumulation was a major contributing factor to the decreased liver weight in αCGRP$^{-/-}$ mice compared with αCGRP$^{+/+}$ mice in the fat-feeding study. Consistent with visual inspection, quantitative measurements and analyses showed that liver triglyceride content was increased in both αCGRP$^{-/-}$ and αCGRP$^{+/+}$ mice administered the 10% fat diet compared with their respective counterparts at baseline (Fig. 6B). In the fat-feeding study, liver triglyceride content was increased in αCGRP$^{-/-}$ mice on the 60% ($P < 0.001$) and 45% ($P < 0.01$) fat diets compared with the control 10% diet and on the 60 *vs.* 45% fat diet ($P < 0.05$) (Fig. 6B). The effect of fat-feeding was also genotype dependent with lower liver triglyceride content in αCGRP$^{-/-}$ mice administered the 10% ($P < 0.001$) and 45% ($P < 0.05$) diets compared with αCGRP$^{+/+}$ mice (Fig. 6B).

Analyses showed that ALT concentrations did not differ between αCGRP$^{+/+}$ and αCGRP$^{-/-}$ mice in the baseline study but were increased by approximately 10-fold in αCGRP$^{+/+}$ mice with age (fat-feeding study) (Fig. 6C). By comparison, in the fat-feeding study, ALT concentrations were lower in αCGRP$^{-/-}$ mice relative to αCGRP$^{+/+}$ mice for all three diets ($P < 0.001$) (Fig. 6C). Plasma concentrations of PAI-1 were also increased in both αCGRP$^{+/+}$ and αCGRP$^{-/-}$ mice in response to the 60% fat diet *vs.* the 45% fat diet ($P < 0.01$) and in response to the 60% fat diet *vs.* the control 10% diet ($P < 0.001$) (Fig. 6D). Nevertheless, overall levels were lower in αCGRP$^{-/-}$ mice compared with αCGRP$^{+/+}$ mice across the three diets ($P < 0.05$) (Fig. 6D). Collectively, these findings demonstrated that the comparative overall reduction in liver triglyceride content in αCGRP$^{-/-}$ mice was associated with improvement in biomarkers of liver function.

Analyses of other terminal serum biomarkers from the fat-feeding study (Supplemental Table 5) revealed a dietary effect on ALP concentrations that was genotype dependent. However, absolute serum ALP concentrations all fell within accepted normal ranges reported for mice (26, 27). Total serum protein concentration was slightly lower

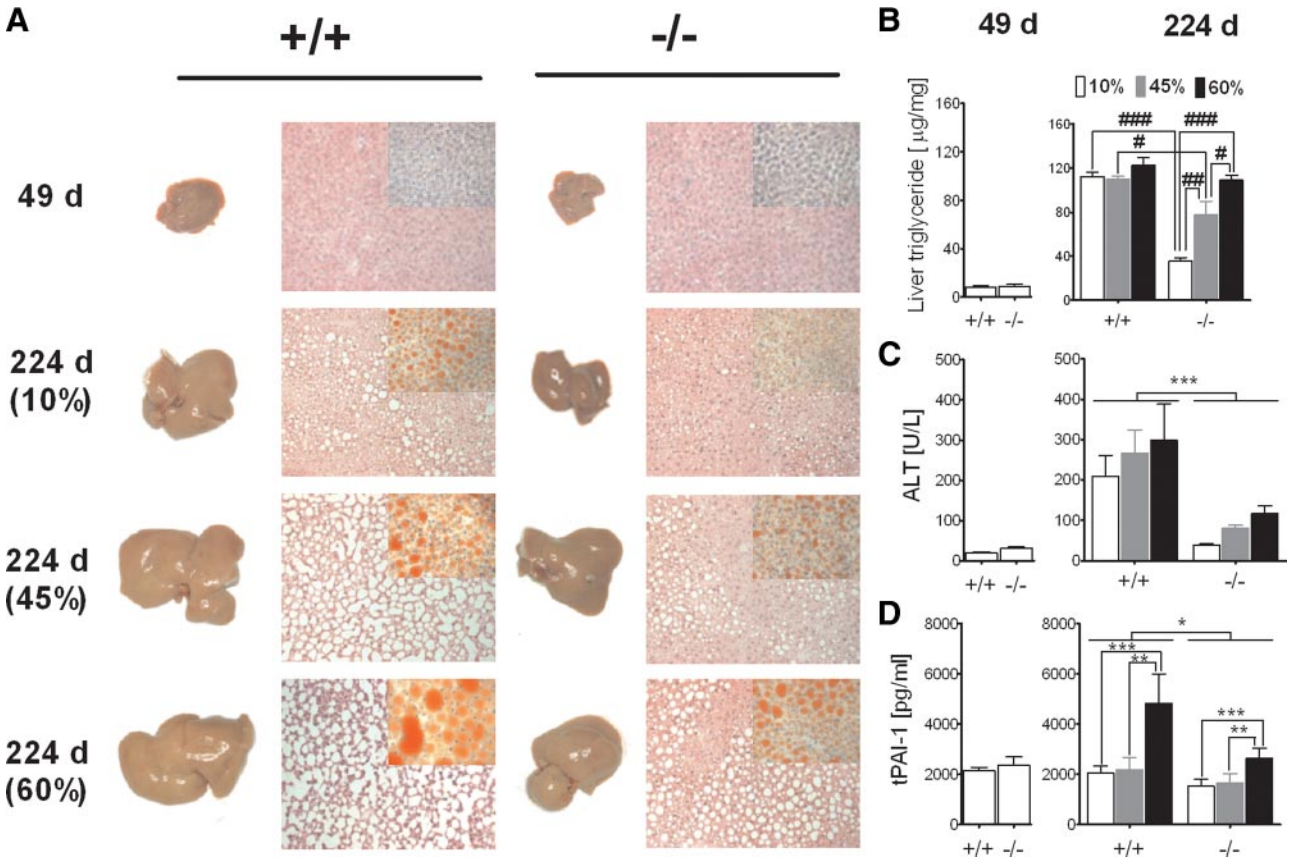

FIG. 6. αCGRP$^{-/-}$ mice display improved liver function and a reduction in triglyceride. A, Whole livers were collected from αCGRP$^{+/+}$ and αCGRP$^{-/-}$ mice at 49 d (baseline study) and at 224 d after feeding regimens comprising control 10, 45, or 60% fat diets (fat-feeding study). Photographs show representative images of livers taken from each group (n = 9–12 mice/group) and corresponding liver tissue sections (6 μm) stained for hemotoxylin and eosin (n = 4–6 mice/group). *Insets*/sections (12 μM) were stained with Oil red-O (n = 4–6 mice/group). B, Liver triglyceride content. C, Serum ALT (n = 9–11 mice/group). D, Total PAI-1 (n = 9–11 mice/group). Values are expressed as mean ± SEM. *, $P < 0.05$; **, $P < 0.01$; ***, $P < 0.001$. Statistical analyses were performed using two-way ANOVA and where a significant genotype ∗ diet interaction was observed, the *post hoc* analyses are represented by *hashed symbols*. #, $P < 0.05$; #, $P < 0.001$.

($P < 0.01$) in αCGRP$^{-/-}$ mice than in αCGRP$^{+/+}$ mice (Supplemental Table 5). Serum free fatty acid concentrations were also significantly increased in response to the 45 and 60% fat diets *vs.* the control 10% fat diet in both αCGRP$^{-/-}$ mice and αCGRP$^{+/+}$ mice. Total serum cholesterol was also increased in αCGRP$^{+/+}$ and αCGRP$^{-/-}$ mice in response to the 45 and 60% fat diets *vs.* the control 10% fat diet (Supplemental Table 5). Nevertheless, total serum cholesterol levels were lower in αCGRP$^{-/-}$ mice compared with αCGRP$^{+/+}$ mice across all three diets. Taken together, these observations showed liver lipid accumulation was associated with an expected impairment in liver function, but that these effects were attenuated in αCGRP$^{-/-}$ mice.

αCGRP$^{-/-}$ mice displayed an overall reduction in adiposity with no evidence for altered immune or thyroid function

Tissue analyses were consistent with overall lower adiposity in αCGRP$^{-/-}$ mice (Supplemental Table 2). There were no significant differences in the thyroid hormones, TSH, and fT4. However, mean serum fT3 concentration was approximately 26% lower ($P < 0.001$) in αCGRP$^{-/-}$ mice than αCGRP$^{+/+}$ mice (Supplemental Table 5), possibly resulting from altered extrathyroidal metabolism. Although TNF-α concentrations in αCGRP$^{-/-}$ mice were increased in the baseline study, there were no significant differences on circulating levels of monocyte chemotactic protein-1 and IL-6 (Supplemental Table 5).

αCGRP$^{-/-}$ mice displayed altered AMPK and acetyl coenzyme A carboxylase (ACC) signaling and expression in liver and skeletal muscle

Analyses of livers taken from 4-h fasted animals in the baseline study revealed increased contents of both phosphorylated AMPK (pAMPK), and phosphorylated ACC (pACC) but not total ACC content in αCGRP$^{-/-}$ mice (Fig. 7A). In the case of pACC, visual inspection of the blots showed that the higher phosphorylated content was due primarily to a 285-kDa protein band consistent with the pACC-2 isoform (Fig. 7A). Total AMPK content was not significantly different (data not shown). In the fat-feeding study, there was no significant change in terminal

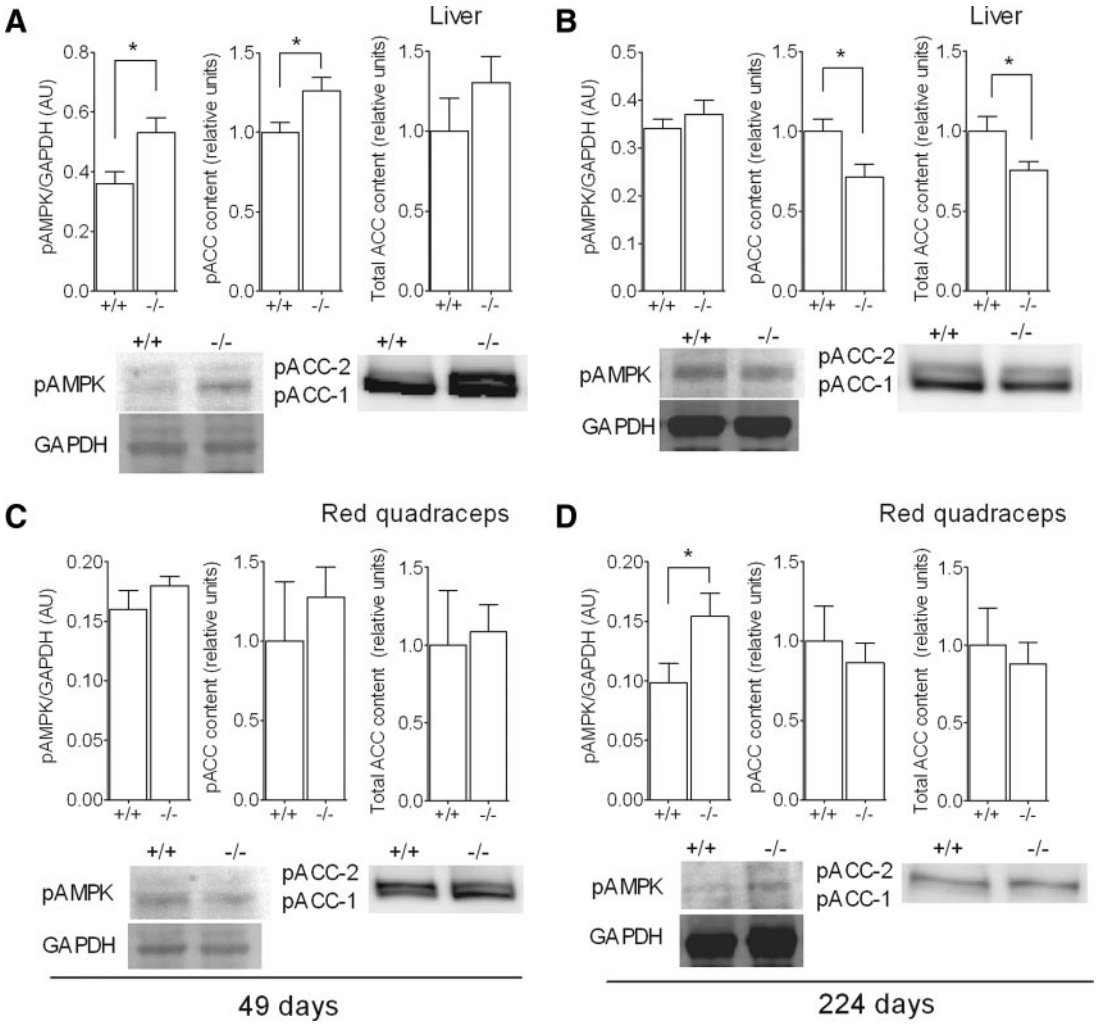

FIG. 7. αCGRP$^{-/-}$ mice display altered AMPK and ACC signaling in liver and red quadriceps muscle. pAMPK and pACC contents were measured in liver (A and B) and red quadriceps muscle (C and D) from αCGRP$^{-/-}$ and αCGRP$^{+/+}$ mice at 49 d (baseline study) and 224 d (fat-feeding study). Values are expressed as mean ± SEM (n = 8 mice/group). Statistical significance was assessed using unpaired *t* tests. *, $P < 0.05$. Phosphorylation and protein levels of AMPK were determined using anti pAMPK and anti-αAMPK antibodies (Cell Signaling, Beverly, MA) and detection using Qdot 605 Goat F(ab')2 antirabbit IgG conjugate (Invitrogen, Carlsbad, CA). Bands were quantified by Gel Doc XR (Bio-Rad, CA) and Quantity One software using glyceraldehyde-3-phosphate dehydrogenase (GAPDH) (Abcam, Cambridge, UK) as a loading control. Phosphorylation and protein levels of ACC were determined using anti pACC and anti-ACC (Cell Signaling) antibodies and immunodetection performed with an enhanced chemoluminescence kit (ECL Plus; GE Healthcare, Amersham, UK).

liver pAMPK or total AMPK (data not shown) content (Fig. 7B). However, both pACC and total ACC contents were lower in αCGRP$^{-/-}$ mice on the control 10% fat diet, indicating decreased ACC protein expression. In red quadriceps muscle, neither pAMPK content nor pACC content differed significantly between αCGRP$^{-/-}$ and αCGRP$^{+/+}$ mice from the baseline study (Fig. 7C). However, terminal pAMPK content was significantly higher in αCGRP$^{-/-}$ mice compared with αCGRP$^{+/+}$ mice on the control 10% fat diet (fat-feeding study) (Fig. 7D). There were no associated changes in either pACC or total ACC contents.

Mitochondrial function was improved in liver and skeletal muscle of αCGRP$^{-/-}$ mice

CS activity was measured in liver and red quadriceps of αCGRP$^{-/-}$ and αCGRP$^{+/+}$ mice. There were no significant differences in maximal CS activity between αCGRP$^{-/-}$ and αCGRP$^{+/+}$ mice in the baseline study in either of these tissues (Fig. 8). However, in the fat-feeding study, CS activity in the liver was lower in αCGRP$^{-/-}$ and αCGRP$^{+/+}$ mice fed the 45% ($P < 0.001$) and 60% ($P < 0.001$) fat diets *vs.* the control 10% fat diet (Fig. 8A). Nevertheless, a small but significant genotype effect was observed ($P < 0.05$), showing increased CS activity in the livers of αCGRP$^{-/-}$ mice across all the diets (Fig. 8A). In red quadriceps muscle, CS activity was increased in both αCGRP$^{-/-}$ and αCGRP$^{+/+}$ mice in response to the 45% ($P < 0.01$) and 60% ($P < 0.01$) fat diets *vs.* the control 10% diet (Fig. 8B). There was also a significant genotype effect ($P < 0.05$), showing increased red quadriceps CS activity in αCGRP$^{-/-}$ mice *vs.* αCGRP$^{+/+}$ mice across all diets (Fig. 8B).

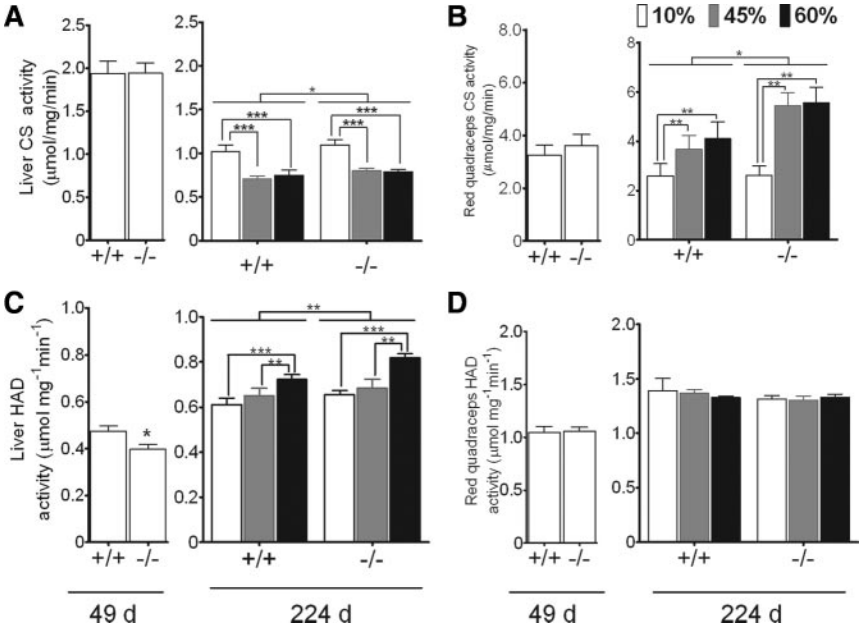

FIG. 8. Enzymatic markers of mitochondrial function in αCGRP$^{+/+}$ and αCGRP$^{-/-}$ mice. CS activities in liver (A), red quadriceps muscle (B), 3-HAD activities in liver (C), and red quadriceps (D) from αCGRP$^{-/-}$ and αCGRP$^{+/+}$ mice at 49 d (baseline study) and 224 d (fat-feeding study). Activities were expressed per milligram of wet tissue weight. Analyses at 49 d were performed on a separate animal cohort (baseline study). Values are expressed as mean ± SEM (n = 5–8 mice/group). *, $P < 0.05$; **, $P < 0.01$; ***, $P < 0.001$.

Corresponding measurements of 3-HAD were decreased in the livers of baseline αCGRP$^{-/-}$ mice ($P < 0.05$) (Fig. 8C). However, in the fat-feeding study, terminal liver 3-HAD activity was increased in αCGRP$^{-/-}$ and αCGRP$^{+/+}$ mice in response to the 60% ($P < 0.01$) fat diets relative to the 45% ($P < 0.01$) and control 10% fat diets ($P < 0.001$) (Fig. 8C). There was also a significant genotype effect ($P < 0.01$), revealing increased 3-HAD activity in αCGRP$^{-/-}$ mice across all diets (Fig. 8C). By contrast, in red quadriceps muscle, there were no significant changes in 3-HAD activity in either the baseline or fat-feeding studies (Fig. 8D).

Mitochondrial DNA copy number also revealed changes in the relative ratio of mitochondrial cytochrome b DNA to the genomic α-globin DNA levels. In the liver of 224 d mice, there was a significant reduction in this ratio in αCGRP$^{+/+}$ mice but not in αCGRP$^{-/-}$ mice on the 60% *vs.* 10% fat diet (Supplemental Fig. 1A). By comparison, in red quadriceps muscle at 224 d, there was a relative reduction in mitochondrial DNA copy number ratio in αCGRP$^{-/-}$ mice compared with control mice (Supplemental Fig. 1B). There was also an effect of the 45% diet on this ratio in αCGRP$^{-/-}$ mice, which was increased compared with the 10 and 60% fat diets (Supplemental Fig. 1B).

Discussion

The genetically susceptible C57BL/6J mouse strain provides a useful model for diet-induced obesity (28). We used this strain to test whether ablation of endogenous αCGRP expression altered obesity-related issues with lipid homeostasis and insulin resistance. In this study, the increased caloric intake in the wild-type αCGRP$^{+/+}$ groups showed the expected increased weight gain, a progressive impairment of glucose handling and insulin sensitivity, hyperinsulinemia, elevated skeletal muscle triglyceride content, and development of fatty livers with perturbed biochemical profiles.

In contrast, the most striking findings were that αCGRP$^{-/-}$ mice displayed lower body weight, improved glucose handling and insulin sensitivity, lower hyperinsulinemia, and lower overall adiposity compared with the αCGRP$^{+/+}$ mice on equivalent diets. Moreover, these improved characteristics were associated with increased overall caloric intakes in αCGRP$^{-/-}$ mice over the fat-feeding trial period. This increased food intake could reflect a physiological role for CGRP in satiety as demonstrated in rats after central administration of the CGRP receptor peptide antagonist, CGRP(8-37), which resulted in an increase in food intake (29).

Accumulation of lipid within the liver is a characteristic of obesity, leading to nonalcoholic fatty liver disease and eventual nonalcoholic steatohepatitis (30). A terminal metabolic snapshot from the fat-feeding study showed that αCGRP$^{-/-}$ mice fed the control diet and the two high-fat diets displayed attenuated symptoms of fatty liver dysfunction, as indicated by lower hepatic triglyceride content, liver mass, and serum ALT concentrations. αCGRP$^{-/-}$ mice also exhibited lower high-density lipoprotein-C and total cholesterol across all diets. Decreased liver triglyceride contents also coincided with an increased β-oxidation marker activity (3-HAD) in liver and lower expression of ACC, an enzyme involved in lipogenesis.

Triglyceride accumulation in skeletal muscle is closely associated with the development of insulin resistance (31). In skeletal muscle, lower triglyceride content in αCGRP$^{-/-}$ mice was associated with higher activities of the mitochondrial marker CS, in response to high-fat feeding compared with αCGRP$^{+/+}$ mice. Notably, CS activity increased in rat skeletal muscle after chronic pharmacological AMPK activation by 5-aminoimidazole-4-carboxamide-1-β-ribofuranoside (32). This suggests that the

higher pAMPK content in red quadriceps of αCGRP$^{-/-}$ mice could be linked to increased CS activity and therefore mitochondrial capacity.

We cannot discount other chronic compensatory background factors, for example, changes in the receptor activity-modifying protein 1 and calcitonin receptor-like receptor subunits that comprise the CGRP receptor (33). However, as indicated by the core body temperature and indirect calorimetery data, increased energy expenditure leading to a lower body weight gain and adiposity best explains the associated metabolic resistance of αCGRP$^{-/-}$ mice to overfeeding. Although we did not include a separate food-restricted animal group to directly test this possibility, our experimental design using two concurrent high-fat diets clearly defined a positive relationship between increased body weight gain and metabolic impairment. In addition, the lower RQ, in conjunction with no apparent change in energy expenditure in αCGRP$^{-/-}$ mice, observed during the less-active daytime indicates elevated β-oxidation flux, and this could also contribute to lower ectopic fat stores.

How could αCGRP mediate these observed effects on energy expenditure? We found no evidence for altered levels of circulating thyroid hormones between knockout and wild-type mice. There is, however, a potential mechanistic link with Aδ- and C-fiber sensory nerves that coexpress CGRP and the heat-sensitive calcium channel receptor, TRPV1. These sensory nerves innervate core body organs, such as the liver (34), brown fat (35), and skeletal muscle (11, 36), and play a role in thermogenesis via regulation of TRPV1 (37). Their stimulation by capsaicin results in hypothermia, whereas TRPV1 antagonists evoke the reverse hyperthermic effects (37). Because CGRP sensory nerve release occurs with activation of TRPV1 (11, 12), it is possible that CGRP acts as a downstream mediator of TRPV1 and could therefore potentially mediate the thermogenic actions of sensory nerves. Consistent with this possibility is the absence of CGRP sensory nerve release in *Trpv1* knockout mice in response to TRPV1 receptor activation (38).

There are strong similarities between our findings and fat-feeding studies in *Trpv1* knockout mice (39). Here, a high-fat diet also resulted in a comparative decrease in body weight gain, adipose mass, and liver lipid droplet size relative to control mice (39). Although *Trpv1*$^{-/-}$ mice displayed similar calorie intakes and dietary lipid absorption, they showed increased thermogenic capacities relative to control mice (39). Similar to our findings with αCGRP$^{-/-}$ mice, the *Trpv1* knockout mice are thought to be leaner due to elevated energy expenditure. Similarities can also be drawn with chronic capsaicin-induced sensory denervation in rats that results in depletion of CGRP and other neuropeptides (40). This study also reported a similar phenotype as with αCGRP$^{-/-}$ mice with decreased body weight gain and adiposity in the face of high-fat diets (41) and improved age-associated insulin resistance (42) and glucose tolerance (43).

Recent evidence suggests that skeletal muscle may act in a thermogenic capacity via mitochondrial uncoupling (44). It is therefore potentially significant that TRPV1-containing CGRP-positive sensory nerve fibers innervate this tissue and may account up to 95% of total CGRP content (36). CGRP is also expressed at the neuromuscular junction of motoneurons and cosecreted with acetylcholine in response to contraction-induced stimuli. It is therefore quite possible that CGRP exerts multiple physiological effects in skeletal muscle, and this may in part explain why incubation of isolated rat soleus muscle with exogenously administered CGRP acutely activates AMPK and increases β-oxidation (23).

In summary, we provide exciting new data showing that αCGRP$^{-/-}$ mice were protected against diet-induced obesity. The attenuated gain in body weight was associated with lower fat storage, lower hepatic lipid accumulation, and a substantial improvement in metabolic health. Before commencement of the fat-feeding study, αCGRP$^{-/-}$ mice also displayed intrinsically higher baseline core body temperature, lipid metabolism, and energy expenditure. The remarkable similarities of this model with the phenotypes of mice with either sensory denervation or disruption of *Trpv1* strongly implicates CGRP as a core mediator of sensory nerve action in energy metabolism. Further, because CGRP secretion from sensory nerves is elevated in preobesity (43), attenuation of αCGRP action may provide new therapeutic opportunities to regulate body weight in obesity.

Acknowledgments

We thank Cynthia Tse for editing and management input and the dedicated staff of the animal facility.

Address all correspondence and requests for reprints to: Kerry M. Loomes, School of Biological Sciences, University of Auckland, Private Bag 92 019, Auckland 1142, New Zealand. E-mail: k.loomes@auckland.ac.nz.

This work was supported by grants from the Endcore Research Trust, the University of Auckland, the Maurice and Phyllis Paykel Trust, the New Zealand Lottery Health Board, Protemix Corp., the Health Research Council of New Zealand (program funding and Ph.D. stipend for S.G.-J.), the Foundation for Research, Science, and Technology (program funding and an enterprise Ph.D. scholarship to C.S.W. cofunded by Protemix Corp.).

Disclosure Summary: The authors have nothing to disclose.

References

1. **Morris HR, Panico M, Etienne T, Tippins J, Girgis SI, MacIntyre I** 1984 Isolation and characterization of human calcitonin gene-related peptide. Nature 308:746–748
2. **Rosenfeld MG, Mermod JJ, Amara SG, Swanson LW, Sawchenko PE, Rivier J, Vale WW, Evans RM** 1983 Production of a novel neuropeptide encoded by the calcitonin gene via tissue-specific RNA processing. Nature 304:129–135
3. **Bovenberg RA, van de Meerendonk WP, Baas PD, Steenbergh PH, Lips CJ, Jansz HS** 1986 Model for alternative RNA processing in human calcitonin gene expression. Nucleic Acids Res 14:8785–8803
4. **Steenbergh PH, Höppener JW, Zandberg J, Lips CJ, Jansz HS** 1985 A second human calcitonin/CGRP gene. FEBS Lett 183:403–407
5. **Kruger L, Mantyh PW, Sternini C, Brecha NC, Mantyh CR** 1988 Calcitonin gene-related peptide (CGRP) in the rat central nervous system: patterns of immunoreactivity and receptor binding sites. Brain Res 463:223–244
6. **Sexton PM, McKenzie JS, Mason RT, Moseley JM, Martin TJ, Mendelsohn FA** 1986 Localization of binding sites for calcitonin gene-related peptide in rat brain by in vitro autoradiography. Neuroscience 19:1235–1245
7. **Skofitsch G, Jacobowitz DM** 1985 Calcitonin gene-related peptide: detailed immunohistochemical distribution in the central nervous system. Peptides 6:721–745
8. **Brain SD, Cambridge H** 1996 Calcitonin gene-related peptide: vasoactive effects and potential theraputic role. Gen Pharmacol 27: 607–611
9. **Gibson SJ, Polak JM, Bloom SR, Sabate IM, Mulderry PM, Ghatei MA, McGregor GP, Morrison JF, Kelly JS, Evans RM, *et al.*** 1984 Calcitonin gene-related peptide immunoreactivity in the spinal cord of man and of eight other species. J Neurosci 4:3101–3111
10. **Takami K, Kawai Y, Uchida S, Tohyama M, Shiotani Y, Yoshida H, Emson PC, Girgis S, Hillyard CJ, MacIntyre I** 1985 Effect of calcitonin gene-related peptide on contraction of striated muscle in the mouse. Neurosci Lett 60:227–230
11. **Leighton B, Foot EA** 1995 The role of the sensory peptide calcitonin-gene-related peptide(s) in skeletal muscle carbohydrate metabolism: effects of capsaicin and resiniferatoxin. Biochem J 307(Pt 3):707–712
12. **Zygmunt PM, Petersson J, Andersson DA, Chuang H, Sørgård M, Di Marzo V, Julius D, Högestätt ED** 1999 Vanilloid receptors on sensory nerves mediate the vasodilator action of anandamide. Nature 400:452–457
13. **Brain SD, Williams TJ, Tippins JR, Morris HR, MacIntyre I** 1985 Calcitonin-gene-related peptide is a potent vasodilator. Nature 313: 54–56
14. **Leighton B, Cooper GJ** 1988 Pancreatic amylin and calcitonin gene-related peptide cause resistance to insulin in skeletal muscle *in vitro*. Nature 335:632–635
15. **Hughes JJ, Levine AS, Morley JE, Gosnell BA, Silvis SE** 1984 Intraventricular calcitonin gene-related peptide inhibits gastric acid secretion. Peptides 5:665–667
16. **Ono K, Delay M, Nakajima T, Irisawa H, Giles W** 1989 Calcitonin gene-related peptide regulates calcium current in heart muscle. Nature 340:721–724
17. **Sala C, Andreose JS, Fumagalli G, Lømo T** 1995 Calcitonin gene-related peptide: possible role in formation and maintenance of neuromuscular junctions. J Neurosci 15:520–528
18. **Harzenetter MD, Novotny AR, Gais P, Molina CA, Altmayr F, Holzmann B** 2007 Negative regulation of TLR responses by the neuropeptide CGRP is mediated by the transcriptional repressor ICER. J Immunol 179:607–615
19. **Fisher LA, Kikkawa DO, Rivier JE, Amara SG, Evans RM, Rosenfeld MG, Vale WW, Brown MR** 1983 Stimulation of noradrenergic sympathetic outflow by calcitonin gene-related peptide. Nature 305:534–536
20. **Oh-hashi Y, Shindo T, Kurihara Y, Imai T, Wang Y, Morita H, Imai Y, Kayaba Y, Nishimatsu H, Suematsu Y, Hirata Y, Yazaki Y, Nagai R, Kuwaki T, Kurihara H** 2001 Elevated sympathetic nervous activity in mice deficient in αCGRP. Circ Res 89:983–990
21. **Schinke T, Liese S, Priemel M, Haberland M, Schilling AF, Catala-Lehnen P, Blicharski D, Rueger JM, Gagel RF, Emeson RB, Amling M** 2004 Decreased bone formation and osteopenia in mice lacking α-calcitonin gene-related peptide. J Bone Miner Res 19:2049–2056
22. **Lu JT, Son YJ, Lee J, Jetton TL, Shiota M, Moscoso L, Niswender KD, Loewy AD, Magnuson MA, Sanes JR, Emeson RB** 1999 Mice lacking α calcitonin gene related peptide exhibit normal cardiovascular regulation and neuromuscular development. Mol Cell Neurosci 14:99–120
23. **Danaher RN, Loomes KM, Leonard BL, Whiting L, Hay DL, Xu LY, Kraegen EW, Phillips AR, Cooper GJ** 2008 Evidence that α-calcitonin gene-related peptide is a neurohormone that controls systemic lipid availability and utilization. Endocrinology 149:154–160
24. **Newsholme EA, Crabtree B** 1986 Maximum catalytic activity of some key enzymes in provision of physiologically useful information about metabolic fluxes. J Exp Zool 239:159–167
25. **Sewell MA** 2005 Utilization of lipids during early development of the sea urchin Evechinus chloroticus. Marine Ecol Progress Series 304:133–142
26. **Frith CH, Suber RL, Umholtz R** 1980 Hematologic and clinical chemistry findings in control BALB/c and C57BL/6 mice. Lab Anim Sci 30:835–840
27. **Harrison Jr SD, Burdeshaw JA, Crosby RG, Cusic AM, Denine EP** 1978 Hematology and clinical chemistry reference values for C57BL/6 X DBA/2 F1 mice. Cancer Res 38:2636–2639
28. **Collins S, Martin TL, Surwit RS, Robidoux J** 2004 Genetic vulnerability to diet-induced obesity in the C57BL/6J mouse: physiological and molecular characteristics. Physiol Behav 81:243–248
29. **Lutz TA, Rossi R, Althaus J, Del Prete E, Scharrer E** 1997 Evidence for a physiological role of central calcitonin gene-related peptide (CGRP) receptors in the control of food intake in rats. Neurosci Lett 230:159–162
30. **Wanless IR, Shiota K** 2004 The pathogenesis of nonalcoholic steatohepatitis and other fatty liver diseases: a four-step model including the role of lipid release and hepatic venular obstruction in the progression to cirrhosis. Semin Liver Dis 24:99–106
31. **McGarry JD** 2002 Banting lecture 2001: dysregulation of fatty acid metabolism in the etiology of type 2 diabetes. Diabetes 51:7–18
32. **Winder WW, Holmes BF, Rubink DS, Jensen EB, Chen M, Holloszy JO** 2000 Activation of AMP-activated protein kinase increases mitochondrial enzymes in skeletal muscle. J Appl Physiol 88:2219–2226
33. **Poyner DR, Sexton PM, Marshall I, Smith DM, Quirion R, Born W, Muff R, Fischer JA, Foord SM** 2002 International Union of Pharmacology. XXXII. The mammalian calcitonin gene-related peptides, adrenomedullin, amylin, and calcitonin receptors. Pharmacol Rev 54:233–246
34. **Tiegs G, Bang R, Neuhuber WL** 1999 Requirement of peptidergic sensory innervation for disease activity in murine models of immune hepatitis and protection by β-adrenergic stimulation. J Neuroimmunol 96:131–143
35. **De Matteis R, Ricquier D, Cinti S** 1998 TH-, NPY-, SP-, and CGRP-immunoreactive nerves in interscapular brown adipose tissue of adult rats acclimated at different temperatures: an immunohistochemical study. J Neurocytol 27:877–886
36. **Sakaguchi M, Inaishi Y, Kashihara Y, Kuno M** 1992 Degeneration of motor nerve fibers enhances the expression of calcitonin gene-related peptide in rat sensory neurons. Neurosci Lett 137:61–64
37. **Steiner AA, Turek VF, Almeida MC, Burmeister JJ, Oliveira DL, Roberts JL, Bannon AW, Norman MH, Louis JC, Treanor JJ, Gavva NR, Romanovsky AA** 2007 Nonthermal activation of transient receptor potential vanilloid-1 channels in abdominal viscera tonically inhibits autonomic cold-defense effectors. J Neurosci 27: 7459–7468

38. **Pethö G, Izydorczyk I, Reeh PW** 2004 Effects of TRPV1 receptor antagonists on stimulated iCGRP release from isolated skin of rats and TRPV1 mutant mice. Pain 109:284–290
39. **Motter AL, Ahern GP** 2008 TRPV1-null mice are protected from diet-induced obesity. FEBS Lett 582:2257–2262
40. **Lundberg JM, Franco-Cereceda A, Alving K, Delay-Goyet P, Lou YP** 1992 Release of calcitonin gene-related peptide from sensory neurons. Ann NY Acad Sci 657:187–193
41. **Cui J, Himms-Hagen J** 1992 Long-term decrease in body fat and in brown adipose tissue in capsaicin-desensitized rats. Am J Physiol 262:R568–R573
42. **Melnyk A, Himms-Hagen J** 1995 Resistance to aging-associated obesity in capsaicin-desensitized rats one year after treatment. Obes Res 3:337–344
43. **Gram DX, Hansen AJ, Wilken M, Elm T, Svendsen O, Carr RD, Ahrén B, Brand CL** 2005 Plasma calcitonin gene-related peptide is increased prior to obesity, and sensory nerve desensitization by capsaicin improves oral glucose tolerance in obese Zucker rats. Eur J Endocrinol 153:963–969
44. **Wijers SL, Schrauwen P, Saris WH, van Marken Lichtenbelt WD** 2008 Human skeletal muscle mitochondrial uncoupling is associated with cold induced adaptive thermogenesis. PLoS One 3:e1777